Creating a Stable Oxide at the Surface of Black Phosphorus

M. T. Edmonds,*[†,‡] A. Tadich,[†,§] A. Carvalho,[∥,⊥] A. Ziletti,[#] K. M. O'Donnell,[□] S. P. Koenig,[∥,⊥] D. F. Coker,[#] B. Özyilmaz,[∥,⊥] A. H. Castro Neto,[∥,⊥,○] and M. S. Fuhrer*[‡,△]

[‡]School of Physics and Astronomy, Monash University, Clayton, Victoria 3800, Australia

[§]Australian Synchrotron, 700 Blackburn Road, Clayton, Victoria 3183, Australia

[∥]Centre for Advanced 2D Materials and Graphene Research Centre and [⊥]Department of Physics, National University of Singapore, Singapore 117546

[#]Department of Chemistry, Boston University, Boston, Massachusetts 02215, United States

[□]Department of Imaging and Applied Physics, Curtin University, Bentley, Western Australia 6102, Australia

[○]Department of Physics, Boston University, Boston, Massachusetts 02215, United States

[△]Center for Nanophysics and Advanced Materials, University of Maryland, College Park, Maryland 207424111, United States

S *Supporting Information*
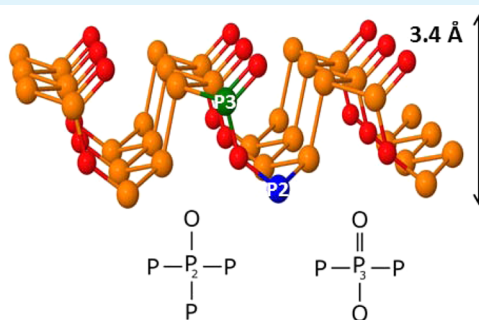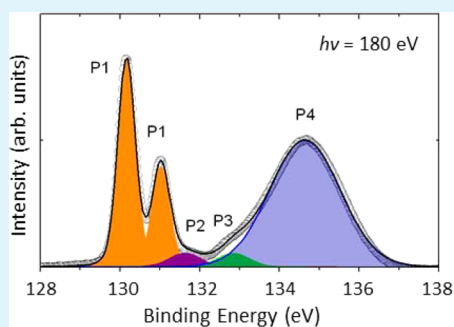
ABSTRACT: The stability of the surface of in situ cleaved black phosphorus crystals upon exposure to atmosphere is investigated with synchrotron-based photoelectron spectroscopy. After 2 days atmosphere exposure a stable subnanometer layer of primarily P_2O_5 forms at the surface. The work function increases by 0.1 eV from 3.9 eV for as-cleaved black phosphorus to 4.0 eV after formation of the 0.4 nm thick oxide, with phosphorus core levels shifting by <0.1 eV. The results indicate minimal charge transfer, suggesting that the oxide layer is suitable for passivation or as an interface layer for further dielectric deposition.

KEYWORDS: air stability, oxidation, black phosphorus, XPS

Black phosphorus is a bulk semiconductor and represents the most thermodynamically stable allotrope of phosphorus,[1] possessing a band gap of ∼0.3 eV[2,3] and a charge carrier mobility of up to 1000 cm^2 V^{-1} s^{-1} at room temperature.[4] As a layered material, mechanical exfoliation has led to the isolation of single and few-layer black phosphorus, known as phosphorene, representing a further addition to the growing family of two-dimensional (2D) materials.[4−6] With a band gap that can be tuned with layer thickness,[7] large exciton binding energy (800 meV),[8,9] high current on/off ratios,[4,10] and ambipolar charge transport,[11] single- and few-layer phosphorene is an attractive candidate for electronic and optoelectronic devices.[5]

Black phosphorus, unlike graphene, which is chemically inert in atmosphere, is expected to oxidize upon exposure to air.[12,13] The formation of surface oxide species has been demonstrated to cause a measurable increase in surface roughness and nonuniform degradation,[10] along with reduced field-effect transistor performance.[14] This presents experimental challenges

for the study of phosphorene-based electronic devices that are prepared and measured in air, because of structural degradation and its effect on the electronic properties. Currently, the focus has been on minimizing the exposure to atmosphere or encapsulating or passivation of phosphorene with air-stable overlayers.[11,14] Yet, the possibility of using a native oxide to deliberately engineer a stable protective layer that protects the pristine layers of black phosphorus below has yet to be explored experimentally. A key motivation to this end is that phosphate glasses are transparent in the ultraviolet (UV) regime,[15] allowing preservation of the large photoresponse observed in phosphorene in the infrared (IR) and UV,[16] making it a suitable platform for optoelectronics.[5]

In the present work, we utilize surface-sensitive photoelectron spectroscopy on black phosphorus crystals cleaved in

vacuum in order to study the chemical changes to the surface resulting from a brief exposure to atmosphere (5 min) followed by longer exposures (up to 28 days). Surface-sensitive photoelectron spectroscopy (photon energy hv = 180 eV) of the P 2p core level allows observation of the evolution of composition at the black phosphorus surface upon air exposure, while low-energy secondary electron cutoff spectroscopy measures the change in work function. We demonstrate that for prolonged air exposure a native phosphorus oxide forms only at the topmost layer of bulk black phosphorus, leaving the deeper layers intact. The oxide growth is found to saturate after 2 days in ambient conditions and consists primarily of phosphorus pentoxide (P_2O_5), with smaller contributions from an intermediate stable oxide p-P_4O_2 consisting of two distinct oxygen−phosphorus moieties: dangling phosphorus−oxygen (O−P=O) and bridging phosphorus−oxygen (P−O−P).[12] The work function of vacuum cleaved black phosphorus is found to be 3.9 eV and increases by only 0.1 eV with the formation of the surface oxide. The realization of a stable oxide layer confined solely to the surface of black phosphorus not only offers protection to the underlying layers, but suggests there is only a minimal effect on the doping of black phosphorus. This makes the native oxide potentially attractive for the subsequent deposition of additional dielectric layers in order to fabricate metal-oxide-semiconductor field-effect transistors.

Figure 1 shows photoelectron spectroscopy measurements of the P 2p core level (hv = 180 eV). In the upper panel of Figure 1 the P 2p core level is depicted after vacuum cleaving without exposure to air, with the subsequent lower panels representing the spectra taken after various exposures to atmosphere. Details on the sample preparation, measurements and peak fitting procedure can be found in the Supporting Information. After cleaving, the phosphorus core level contains only the characteristic doublet representing the P $2p_{3/2}$ and P $2p_{1/2}$ orbitals with peak positions of 130.06 and 130.92 eV respectively, with a Gaussian width of 0.21 eV and Lorentz width of 0.08 eV. These peaks are labeled P1, corresponding to phosphorus−phosphorus bonds within black phosphorus. The spin-splitting of 0.86 eV remains fixed in all subsequent peak fitting of the bulk black phosphorus components. After a 5 min air exposure (not shown in Figure 1) no change was observed in the P 2p core level apart from a slight shift to higher binding energy of 0.10 eV. This is consistent with a shift of the Fermi level toward the conduction band that may be a result of hydrogen defects due to the formation of phosphoric acid on the surface or physisorbed oxygen and nitrogen.[17] After 1 day air exposure, the P1 component shifts back to lower binding energy by 0.08 eV along with an increase in the Gaussian width to 0.48 eV (this width remained constant for the subsequent longer exposure periods). This shift back in binding energy is consistent with transport measurements performed on black phosphorus as a function of exposure time to atmosphere.[17] This is accompanied by the emergence of three new components within the P 2p core level, all to higher binding energy of P1, and which are related to the oxidation occurring at the surface. Following the convention for peak fitting the broader nature of oxide-derived spin-split core levels, a single Voigt function rather than a doublet has been used.[18,19] The first two components labeled P2 and P3 are of equal peak area and located at 131.54 and 132.67 eV, respectively. The third component labeled P4 represents the most dominant oxide component and appears at 134.46 eV, and has a peak area ratio
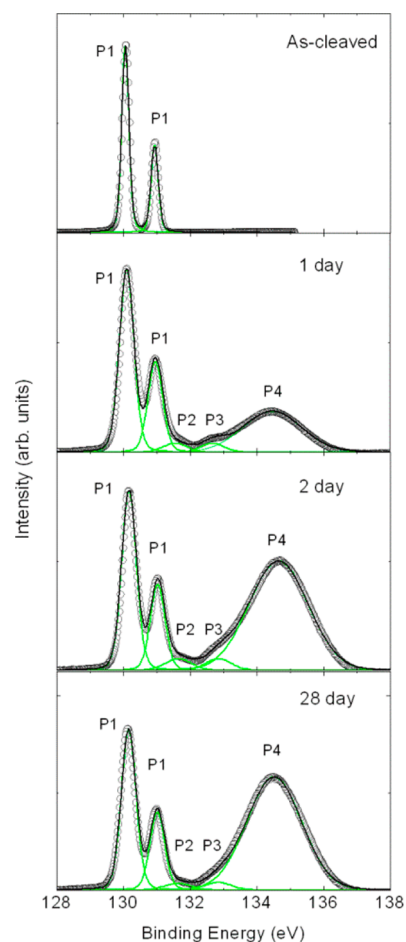

Figure 1. Evolution of cleaved black phosphorus after exposure to atmospheric conditions. P 2p core level spectra of black phosphorus taken at 180 eV where from top to bottom the panels correspond to the as-cleaved surface, 1 day, 2 day, and 28 day air-exposure. P1 represents phosphorus bonded to phosphorus, and P2, P3, and P4 represent the different oxide species as described in the text.

relative to P2 and P3 of ∼11. Moving to the longer 2 day exposure, the P 2p spectra show a significant increase in the intensity of P4, whereas P2 and P3 remain relatively constant; the peak area ratio of P4 to the smaller peaks now increases to 20. Finally, after 28 days exposure to atmosphere the P 2p spectra shows minimal changes compared to the 2 day exposure, indicating that the growth of the phosphorus oxide saturates after approximately 2 days in air. For the prolonged exposure periods, further XPS scans (not shown) reveal that a significant amount of adventitious carbon species have physisorbed onto the surface, along with a small amount of nitrogen. As neither of these species are expected to chemically bond to black phosphorus, the presence of these adsorbed species does not alter our interpretation of the surface oxidation.

In the upper panel of Figure 2a we plot the P 2p spectra for the 2 day air exposure taken at hv = 180 eV, where P1, P2, P3, and P4 are shown as orange, purple, green, and blue, respectively. The binding energy separation of the P2, P3 and P4 oxide components from the P $2p_{3/2}$ component of P1 is 1.48 eV, 2.68, and 4.48 eV respectively. This sequential shift to higher binding energy of these components represents an increasing deficiency in electron density around the phosphorus atom and stronger charge localization around the oxygen. To
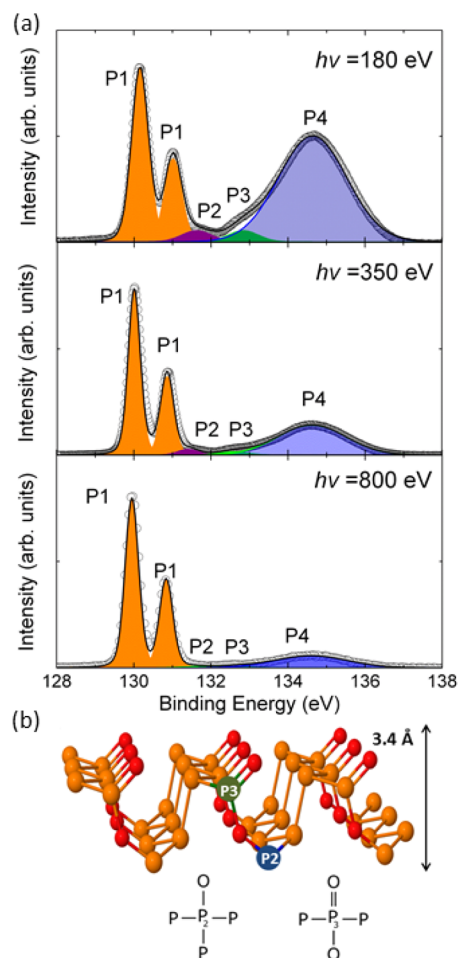
Figure 2. (a) Depth-dependent photoelectron spectroscopy of the P 2p core level of black phosphorus after 2 days air exposure taken at $h\nu$ = 180 eV (upper panel), 350 eV (middle panel) and 800 eV (lower panel). (b) Structural model of p-P_4O_2 where P2 and P3 represent P–O–P and O–P=O bonding configurations, respectively, along with ball and stick representations of the surrounding atoms to P2 and P3.

determine the origin of the three oxide components we examine the various stable bonding configurations of oxidized black phosphorus. The first structural model chosen is an intermediate stable oxide p-P_4O_2 containing two oxygen–

phosphorus moieties: dangling phosphorus–oxygen (O–P=O) and bridging phosphorus–oxygen (P–O–P) as shown in Figure 2(b).[12] DFT calculations were then performed on this structure in order to simulate the XPS P 2p core level shifts with respect to pristine black phosphorus (details in Supporting Information). For p-P_4O_2 the calculated separations between the bulk black phosphorus P 2p core level and the bridging (P–O–P) and dangling (O–P=O) motifs are 1.38 and 2.3 eV, respectively, close to the experimental values of P2 (1.48 eV) and P3 (2.68 eV). We therefore assign P2 to bridging (P–O–P) and P3 to dangling (O–P=O) bonding environments. Turning to the assignment of P4, the large separation of 4.48 eV from the bulk black phosphorus P $2p_{3/2}$ component clearly shows that this component represents a phosphorus species bonded to an even larger number of oxygen atoms than either P2 or P3. Phosphorus pentoxide (P_2O_5) contains four oxygen atoms bonded to each phosphorus site; representing the most oxygen-saturated form of phosphorus oxide. Literature values of P_2O_5 report binding energies between 134.5 eV[20] and 135.0 eV,[21] in good agreement with our value of 134.65 eV for the 2 day air exposure which represents the saturated surface. This value is also in good agreement with the simulated XPS P 2p core level shift predicted by DFT calculations on the P_2O_5 structure of 5.0 eV. Therefore, we assign P4 to phosphorus–oxygen bonds in P_2O_5. The results clearly show that prolonged air exposure of in situ cleaved black phosphorus causes the surface to oxidize to form predominantly P_2O_5, and small regions of intermediate oxidation composed of the P–O–P and O–P=O motifs, as for example the p-P_4O_2 form shown in Figure 2b.

With the identification of all oxide components now complete, we turn to whether the oxidation is confined to the surface of black phosphorus, or has penetrated deeper into the bulk. To achieve this, we measured the P 2p core level using larger photon energies up to 800 eV in order to increase the photoelectron mean free path and therefore the sampling depth of the experiment. In Figure 2a, the P 2p core level spectra, after 2 days air exposure are plotted at 180 eV (upper panel), 350 eV (middle panel) and 800 eV (lower panel). As the photon energy increases (i.e., the emitted photoelectrons possess a larger kinetic energy) the intensity of the oxide components relative to the bulk black phosphorus decreases. Because of the larger mean free path of the emitted photoelectrons, this demonstrates that the formation of
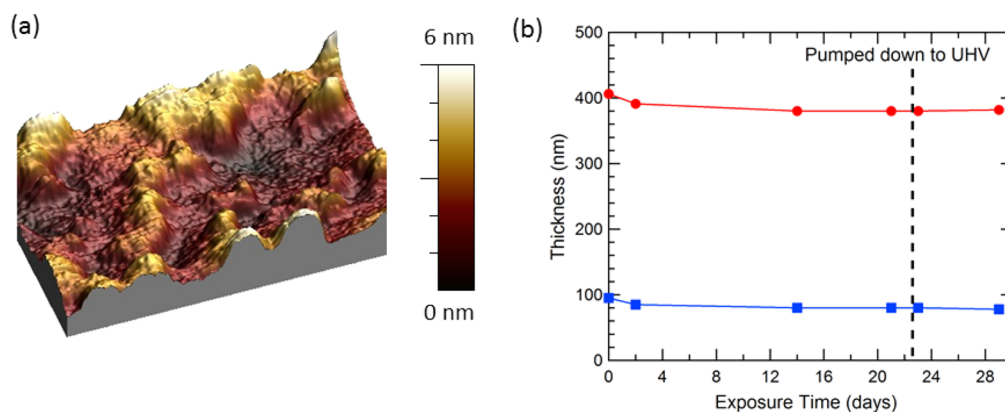

Figure 3. (a) AFM topography image (500 nm × 500 nm) of oxidized black phosphorus with an RMS roughness of 1.5 nm. (b) Thickness of two exfoliated black phosphorus flakes on SiO_2/Si as a function of exposure time, where red circles represent a 406 nm as-cleaved flake and blue squares represent a 95 nm as-cleaved flake.

phosphorus oxide is confined to the surface of black phosphorus, with little if any oxidation of the bulk. The thickness of the phosphorus oxide can be estimated from the peak area ratio of the black phosphorus and phosphorus oxide components using the relation $d = \lambda \ln(I_{Oxide}/I_{BP} + 1)$ where λ is the photoelectron mean free path, and I_{BP} and I_{Oxide} represent the peak area of the bulk black phosphorus and oxide components, respectively.[22,23] From the 180, 350, and 800 eV spectra taken after 2 days air exposure in Figure 2a (i.e., the saturated oxide coverage), we determine an average thickness of the phosphorus oxide of 0.40 ± 0.3 nm. This value is in good agreement with the calculated value of 0.46 nm for a single layer of planar P_2O_5 calculated using DFT,[12] and confirms that only the top layer of black phosphorus has become oxidized.

The observation of a thin stable oxide is surprising in light of previous AFM studies that have observed significant surface roughening of few-layer exfoliated phosphorene on exposure to air.[14,17] To further investigate the effect of air exposure on the surface morphology, we performed atomic force microscopy in tapping mode on a black phosphorus crystal that had been in situ cleaved and then exposed to atmospheric conditions for more than 28 days. Figure 3a shows a three-dimensional plot of the surface morphology (500 nm × 500 nm) of air exposed black phosphorus, which exhibits a RMS surface roughness of ~1.5 nm. In a different region of the sample, a similar RMS roughness of 2.0 nm was also measured. A black phosphorus sample was also measured immediately after ex situ cleaving in ambient conditions, yielding an RMS surface roughness of ~0.8 nm. This increased surface roughness is qualitatively consistent with previous studies that reported an increase in surface roughness upon exposure to atmosphere as a result of oxide formation.[10] However, this lateral uniformity in roughness of our oxidized surface stands in contrast to the large islands or "bubbles" (possibly water droplets) of approximately 5−20 nm in height reported elsewhere.[14,17,24] The absence of these large, thick islands further corroborates our photoelectron spectroscopy observations that the oxide is related to the black phosphorus surface and is relatively uniform. Furthermore, it helps to explain the significant broadening of the Gaussian width that occurs for air exposure of 1 day or more, as the increased surface roughness and nonuniform surface potential is expected to result in increased photoelectron scattering. One possible explanation for the absence of bubbles is that previous AFM studies have measured few-layer black phosphorus, whereas we study bulk black phosphorus samples. For both black phosphorus and also MoS_2, it has been shown that fewer adsorbed water bubbles are observed on the surface with increasing layer thickness, as a result of decreased wettability.[17,25] Another possibility is that the oxide formation results in stress and causes buckling in thin films of phosphorene, observed as "bubbles".

One possible alternative to the formation of a stable oxide is that the black phosphorus is continually etched away as a result of phosphoric acid produced during oxidation, with the phosphoric acid being removed (and thus not apparent) by evaporation either in ambient or when the sample is placed in vacuum for XPS measurements. To rule this out, we used AFM to measure the change in thickness of exfoliated black phosphorus flakes as a function of exposure time. Figure 3b plots the change in thickness of two black phosphorus flakes exfoliated onto a 290 nm SiO_2/Si substrate, where the red circles and blue squares represent 406 nm (flake 1) and 95 nm (flake 2) as-cleaved flakes, respectively. Both flakes undergo

significant etching after 2 day exposure, with a reduction in thickness of 15 and 10 nm for flake 1 and 2, respectively. The etching saturates at 14 days, with no further etching occurring after an additional 1 week air exposure. At 23 days exposure, the samples were subsequently introduced into vacuum and pumped down to 4×10^{-7} mbar for 1 h before being taken out and remeasured (indicated by the dashed line in Figure 3b). No change in thickness was observed immediately after re-exposure to atmosphere or after a further 6 days air exposure. This initial etching of black phosphorus is consistent with previous reports on thin phosphorene flakes.[16] Importantly, however, this saturation is quantitatively consistent with the photoelectron spectroscopy results that demonstrate the formation of a stable oxide layer rather than a continuous etching mechanism due to phosphoric acid.

We now turn to measurements of the valence band and work function in order to understand the band alignment of black phosphorus and phosphorus oxide. Figure 4a plots the valence band (taken at $hv = 100$ eV) for the as-cleaved surface (black) and 2 days air exposure (red). The spectrum obtained for the in situ cleaved surface is in good agreement with previous reports.[26,27] The inset of Figure 4a plots the joint density-of-states close to the Fermi level, where the sharp onset in intensity observed at 40 meV below the Fermi level corresponds to the valence band maximum (i.e., $E_F - E_{VBM} = 40 \pm 50$ meV), in excellent agreement with ref 26. From this we determine a fixed separation of the valence band maximum to the P $2p_{3/2}$ orbital of 130.02 ± 0.05 eV. The spectra for the 2 day exposure shows a large suppression in the valence band features corresponding to black phosphorus, along with the emergence of a new structure ~4 eV below the Fermi level. This feature corresponds to the valence band of phosphorus oxide, and allows us to determine a position of the valence band maximum of phosphorus oxide relative to the Fermi level of 4.2 ± 0.2 eV (i.e., $E_F - E_{VBM} = 4.2 \pm 0.2$ eV), which is consistent with previous measurements on layered forms of P_2O_5.[21]

In Figure 4b, the secondary electron yield vs photoelectron kinetic energy is plotted for as-cleaved (black), 1 day (blue), 2 day (green), and 28 day (red) exposure times. The onset in the secondary electron yield corresponds to the vacuum level of the sample with respect to the Fermi energy, and thus directly yields the work function. For the vacuum cleaved black phosphorus, the work function is 3.9 ± 0.05 eV, and upon air exposure the position of the cutoff changes by only 0.1 eV and eventually reaches a saturated value after 2 days air exposure of 4.0 ± 0.05 eV. The overall yield of secondary electrons increases 5-fold from the as-cleaved to the 28 day spectra; this increase is most likely due to a decrease in the electron affinity upon surface oxidation. The electron affinity of the as-cleaved black phosphorus is 3.6 ± 0.1 eV calculated using $\chi = \phi + (E_F - E_{VBM}) - E_{GAP}$, where $\phi = 3.9$ eV, $E_F - E_{VBM} = 40$ meV, and $E_{GAP} = 0.3$ eV.[2] The decrease in electron affinity implies a bandgap of oxidized black phosphorus which significantly exceeds the measured $E_F - E_{VBM} = 4.2 \pm 0.2$ eV. This is consistent with the theoretical calculations that find there is a substantial increase of the bandgap energy to between 8.5 and 8.7 eV for the different polymorphs of P_2O_5.[12] However, since we cannot determine the exact planar polymorph via XPS, it is not possible to establish an exact value for the electron affinity of the oxidized surface. To summarize our experimental results, the energy level diagrams of the as-cleaved black phosphorus and the oxidized surface after 2 days air exposure are shown in
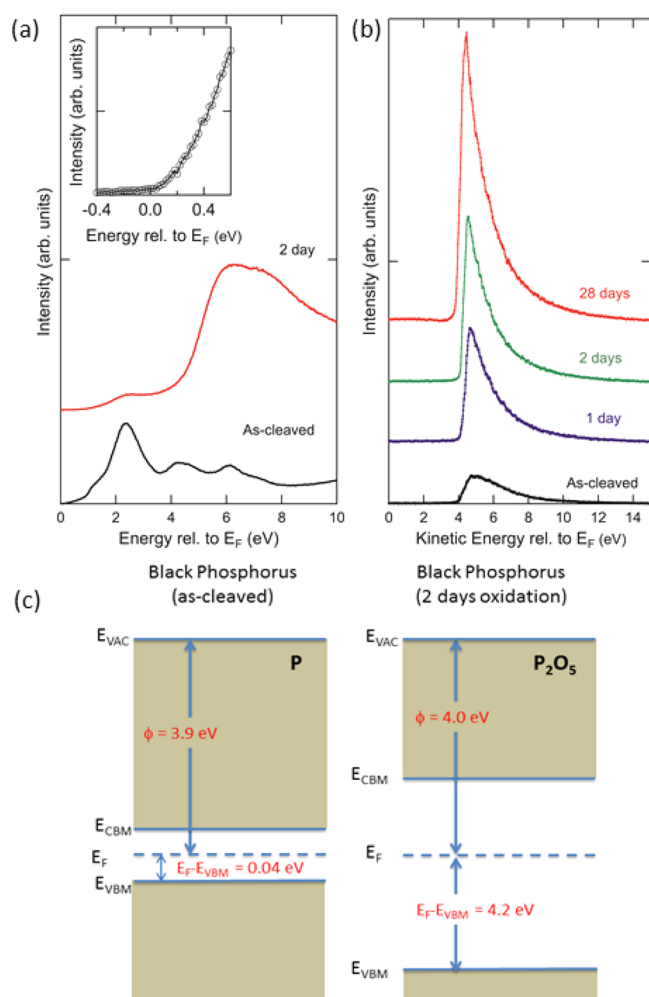
Figure 4. Valence band and low energy cutoff measurements of in situ cleaved black phosphorus after exposure to air. (a) Angle-integrated valence band spectra for as-cleaved black phosphorus (black) and after two-days air exposure (red). Inset: Zoom in of the valence band structure close to the Fermi level for the as-cleaved surface. (b) Secondary electron cutoff as a function of air-exposure for the as-cleaved (black), 1 day air-exposure (blue), 2 day air-exposure (green), and 28 day air-exposure (red). (c) Band level diagrams of black phosphorus for as-cleaved (left panel) and after 2 days oxidation (right panel).

Figure 4c, where the left panel represents the as-cleaved surface and the right panel the oxidized surface.

In conclusion, we have demonstrated that a stable single-layer oxide forms at the surface of black phosphorus after 2 days of exposure to air. By performing surface-sensitive photoelectron spectroscopy, three types of local phosphorus–oxygen environments are identified in the P 2p core level. It is found that the majority of the oxide is made up of phosphorus pentoxide, which represents the most thermodynamically stable oxidation pathway. The demonstration that phosphorus oxide only forms at the top layer of bulk black phosphorus offers great potential as a stable and protective capping layer. Furthermore, the stable phosphorus oxide layer can be used for optoelectronic devices utilizing black phosphorus or few-layer phosphorene because of its transparency in the UV. Finally, the closely matching work functions of black phosphorus and phosphorus oxide, and small ($\leq$100 meV) shift of the P 2p core levels upon oxidation, indicate only a small amount of charge transfer between the oxide and underlying black phosphorus layers. We conclude that the native oxide formed on black phosphorus is a stable passivation layer with minimal effect on the doping of black phosphorus. The native oxide is also potentially attractive for the subsequent deposition of additional dielectric layers in order to fabricate metal-oxide-semiconductor field-effect structures.

■ ASSOCIATED CONTENT

Ⓢ Supporting Information

Additional information on the experimental methods including the photoelectron spectroscopy measurements and the density functional theory calculations. The Supporting Information is available free of charge on the ACS Publications website at DOI: 10.1021/acsami.5b01297.

■ AUTHOR INFORMATION

Corresponding Authors
*E-mail: michael.fuhrer@monash.edu.
*E-mail: mark.edmonds@monash.edu.

Author Contributions
†M.T.E. and A.T. contributed equally to this work

Notes
The authors declare no competing financial interest.

■ ACKNOWLEDGMENTS

■ REFERENCES

(1) Jamieson, J. C. Crystal Structures Adopted by Black Phosphorus at High Pressures. *Science* **1963**, *139*, 1291−1292.

(2) Keyes, R. W. The Electrical Properties of Black Phosphorus. *Phys. Rev.* **1953**, *92*, 580−584.

(3) Takao, Y.; Asahina, H.; Morita, A. J. Electronic Structure of Black Phosphorus in Tight Binding Approach. *J. Phys. Soc. Jpn.* **1981**, *50*, 3362−3369.

(4) Li, L.; Yu, Y.; Ye, G. J.; Ge, Q.; Ou, X.; Wu, H.; Feng, D.; Chen, X. H.; Zhang, Y. Black Phosphorus Field-Effect Transistors. *Nat. Nanotechnol.* **2014**, *9*, 372−377.

(5) Xia, F.; Wang, H.; Jia, Y. Rediscovering Black Phosphorus as an Anisotropic Layered Material for Optoelectronics and Electronics. *Nat. Commun.* **2014**, *5*, 4458−4463.

(6) Castellanos-Gomez, A.; Vicarelli, L.; Prada, E.; Island, J. O.; Narasimha-Acharya, K. L.; Blanter, S. I.; Groenendijk, D. J.; Buscema,

M.; Steele, G. A.; Alvarez, J. V.; Zandbergen, H. W.; Palacios, J. J.; van der Zant, H. S. J. Isolation and Characterization of Few-Layer Black Phosphorus. *2D Mater.* **2014**, *1*, 025001−025020.

(7) Qiao, J.; Kong, X.; Hu, Z.-X.; Yang, F.; Ji, W. High-mobility Transport Anisotropy and Linear Dichroism in Few-Layer Black Phosphorus. *Nat. Commun.* **2014**, *5*, 4475−4481.

(8) Tran, V.; Soklaski, R.; Liang, Y.; Yang, L. Layer-controlled Band Gap and Anisotropic Excitons in Few-layer Black Phosphorus. *Phys. Rev. B* **2014**, *89*, 235319−235324.

(9) Rodin, A.; Carvalho, A.; Castro Neto, A. H. Excitons in Anisotropic Two-dimensional Semiconducting Crystals. *Phys. Rev. B* **2014**, *90*, 075429−075435.

(10) Koenig, S. P.; Doganov, R. A.; Schmidt, H.; Castro Neto, A. H.; Özyilmaz, B. Electric Field Effect in Ultrathin Black Phosphorus. *Appl. Phys. Lett.* **2014**, *104*, 103106−103109.

(11) Doganov, R. A.; O'Farrell, E. C. T.; Koenig, S. P.; Yeo, Y.; Ziletti, A.; Carvalho, A.; Campbell, D. K.; Coker, D. F.; Watanabe, K.; Taniguchi, T.; Castro Neto, A. H.; Öezyilmaz, B. Transport Properties of Pristine Few-Layer Black Phosphorus by Van der Waals Passivation in Inert Atmosphere. *Nat. Commun.* **2015**, *6*, 6647−6653.

(12) Ziletti, A.; Carvalho, A.; Trevisanutto, P. E.; Campbell, D. K.; Coker, D. F.; Castro Neto, A. H. Phosphorene Oxides: Bandgap Engineering of Phosphorene by Oxidation. *Phys. Rev. B* **2015**, *91*, 085407−085416.

(13) Ziletti, A.; Carvalho, A.; Campbell, D. K.; Coker, D. F.; Castro Neto, A. H. Oxygen Defects in Phosphorene. *Phys. Rev. Lett.* **2015**, *114*, 046801−046805.

(14) Wood, J. D.; Wells, S. A.; Jariwala, D.; Chen, K.-S.; Cho, E.; Sangwan, V. K.; Liu, X.; Lauhon, L. J.; Marks, T. J.; Hersam, M. C. Effective Passivation of Exfoliated Black Phosphorus Transistors against Ambient Degradation. *Nano Lett.* **2014**, *14*, 6964−6970.

(15) Brow, R. K. The Structure of Simple Phosphate Glasses. *J. Non-Cryst. Solids* **2000**, *263−264*, 1−28.

(16) Buscema, M.; Groenendijk, D. J.; Blanter, S. I.; Steele, G. A.; van der Zant, H. S. J.; Castellanos-Gomez, A. Fast and Broadband Photoresponse of Few-layer Black Phosphorus Field-Effect Transistors. *Nano Lett.* **2014**, *14*, 3347−3352.

(17) Island, J. O.; Steele, G. A.; van der Zant, H. S. J.; Castellanos-Gomez, A. Environmental Instability of Few-Layer Black Phosphorus. *2D Mater.* **2015**, *2*, 011002−011007.

(18) Ong, C. W.; Huang, H.; Zheng, B.; Kwok, R. W. M.; Hui, Y. Y.; Lau, W. M. X-ray Photoemission Spectroscopy of Nonmetallic Materials: Electronic Structures of Boron and B_xO_y. *J. Appl. Phys.* **2004**, *95*, 3527−3534.

(19) Bagus, P. S.; Ilton, E. S.; Nelin, C. J. The Interpretation of XPS Spectra: Insights into Materials Properties. *Surf. Sci. Rep.* **2013**, *68*, 273−304.

(20) Kim, K.-K.; Kim, H.-S.; Hwang, D.-K.; Lim, J.-H.; Park, S.-J. Realization of p-type ZnO Thin Films via Phosphorus Doping and Thermal Activation of the Dopant. *Appl. Phys. Lett.* **2003**, *83*, 63−65.

(21) Gaskell, K. J.; Smith, M. M.; Sherwood, P. M. A. Valence Band X-ray Photoelectron Spectroscopic Studies of Phosphorus Oxides and Phosphates. *J. Vac. Sci. Technol. A* **2004**, *22*, 1331−1336.

(22) Edmonds, M. T.; Hellerstedt, J.; Tadich, A.; Schenk, A.; O'Donnell, K. M.; Tosado, J.; Butch, N. P.; Syers, P.; Paglione, J.; Fuhrer, M. S. Stability and Surface Reconstruction of Topological Insulator Bi_2Se_3 on Exposure to Atmosphere. *J. Phys. Chem. C* **2014**, *118*, 20413−20419.

(23) Zangwill, A. *Physics at Surfaces*, 1st ed; Cambridge University Press: Cambridge, U.K., 1988.

(24) Yau, S.-L.; Moffat, T. P.; Bard, A. J.; Zhang, Z.; Lerner, M. M. STM of the (010) Surface of Orthorhombic Phosphorus. *Chem. Phys. Lett.* **1992**, *198*, 383−388.

(25) Sahoo, A.; Gaur, A. P. S.; Ahmadi, M.; Guinel, M. J. F.; Katiyar, R. S. Temperature-dependent Raman Studies and Thermal Conductivity of Few-layer MoS_2. *J. Phys. Cem. C* **2013**, *117*, 9042−9047.

(26) Han, C. Q.; Yao, M. Y.; Bai, X. X.; Miao, L.; Zhu, F.; Guan, D. D.; Wang, S.; Gao, C. L.; Liu, C.; Qian, D. Electronic Structure of Black Phosphorus Studied by Angle-resolved Photoemission Spectroscopy. *Phys. Rev. B* **2014**, *90*, 085101−085105.

(27) Taniguchi, M.; Suga, S.; Seki, M.; Sakamoto, H.; Kanzaki, H.; Akahama, Y.; Terada, S.; Endo, S.; Narita, S. Valence Band and Core-level Photoemission Spectra of Black Phosphorus Single Crystals. *Solid State Commun.* **1983**, *45*, 59−61.